Coordination of Autonomous Vehicles and Dynamic Traffic Rules in Mixed Automated/Manual Traffic

Firoozi, Roya; Quirynen, Rien; Di Cairano, Stefano

Abstract

We consider the coordination of multiple con- nected automated vehicles (CAVs) by a central coordinator (CC) in mixed traffic where also non-controlled vehicles (NCVs) are present. The CC directly provides motion target commands to the CAVs and affects the behavior of NCVs by controlling dynamic traffic rules, such as changing traffic lights. We model the traffic rules for these scenarios by mixed-logical constraints, and the response of the NCVs to the changing traffic rules by a switched system with switches triggered by logic conditions. The proposed approach is implemented as a mixed-integer programming (MIP) problem to be solved in the central coordinator, which also handles timing constraint

American Control Conference (ACC) 2022

Coordination of Autonomous Vehicles and Dynamic Traffic Rules in Mixed Automated/Manual Traffic

Roya Firoozi, Rien Quirynen, Stefano Di Cairano

Abstract— We consider the coordination of multiple connected automated vehicles (CAVs) by a central coordinator (CC) in mixed traffic where also non-controlled vehicles (NCVs) are present. The CC directly provides motion target commands to the CAVs and affects the behavior of NCVs by controlling dynamic traffic rules, such as changing traffic lights. We model the traffic rules for these scenarios by mixed-logical constraints, and the response of the NCVs to the changing traffic rules by a switched system with switches triggered by logic conditions. The proposed approach is implemented as a mixed-integer programming (MIP) problem to be solved in the central coordinator, which also handles timing constraints.

I. INTRODUCTION

Connectivity between vehicles can greatly reduce the challenges for autonomous driving (AD) systems, especially when supported by a smart infrastructure system that can provide information to and coordination of the automated vehicles [1]. In recent works, we explored the impact of smart infrastructure that can provide coordination of automated vehicles in challenging scenarios, such as merging points [2] and intersections [3], and in limited access areas such as production or storage sites [4]. In such systems, a central coordinator operating on a mobility edge computing (MEC) platform, significantly more powerful than the vehicle embedded processors [5], performs a centralized decision making for all the automated vehicles and provides the motion plan targets for each single vehicle.

Guaranteeing a proper interaction of automated vehicles with manual vehicles is of paramount importance for AD systems. In [4], we considered the presence of both connected automated vehicles (CAVs) and non-controlled vehicles (NCVs), i.e., manually-operated. Since the central coordinator only affected CAVs, NCVs were always given priority. In the present paper, we consider a central coordinator that can directly control CAVs, and indirectly affect NCVs by dynamically changing traffic rules, such as traffic lights and variable speed limits, as shown in Fig. 1.

Some prior research on CAVs used traffic light timing to improve fuel economy, see, e.g., [6], [7], while control of traffic lights was primarily explored for conventional traffic flow control, see, e.g., [8], [9]. Here, we develop a central coordinator (CC) that actively controls the CAVs by providing targets to the on-board motion planner, together with the traffic lights to affect NCVs and hence optimize the behavior of all vehicles.

The authors are with the Mitsubishi Electric Research Laboratories, Cambridge, MA, 02139, USA {firoozi, quirynen, dicairano}@merl.com.
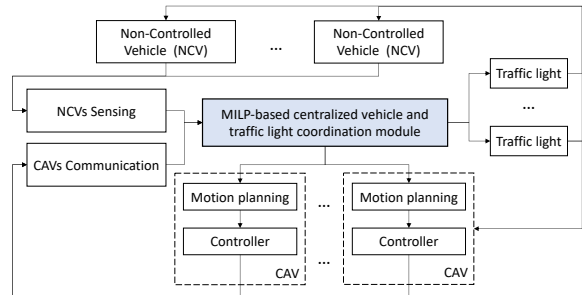
Fig. 1. Schematic of the proposed central coordinator directly controlling connected automated vehicles (CAVs) and indirectly affecting motion of non-controlled vehicles (NCVs) by commanding traffic lights.

With respect to [4], we establish a switching model that represents the reaction of the NCVs to the dynamic traffic rules. Because of that, and to handle timers associated with such traffic rules, we step from an event-driven formulation to a discrete-time representation, which also enables more complex vehicle motion models, and considering multi-lane roads. The resulting coordinator solves a mixed-integer programming (MIP) problem where many of the binary variables are fixed by the initial conditions of the vehicles, so that the actual computation time remains tractable.

In Section II we describe the CAVs and NCVs coordination with dynamic traffic rules, in Section III the general formulation for such a problem, and in Section IV some implementation aspects for a specific class of motion models and rules. Section V reports some simulation results and Section VI discusses the conclusions.

Notation: $\mathbb{R}$, $\mathbb{R}_{0+}$, $\mathbb{R}_+$ ($\mathbb{Z}$, $\mathbb{Z}_{0+}$, $\mathbb{Z}_+$) are the set of real, positive real and nonnegative real (integer) numbers, and $\mathbb{B} = \{0, 1\}$. The logical operators *and*, *or*, *xor*, *not* are $\wedge$, $\vee$, $\underline{\vee}$, $\neg$, and the logical operators *implies* and *equivalent (if and only if)* are $\implies$, $\iff$. For a discrete time signal $x(t)$ sampled with period T_s, $x(k|t)$ is the value of x predicted k steps ahead of t, based on data at step t. Inequalities between vectors are intended componentwise.

II. PROBLEM DESCRIPTION

We design a central coordinator (CC) for the motion of a set of controlled autonomous vehicles (CAVs) through a sequence of roads and intersections, possibly with multiple lanes, where also non-controlled vehicles (NCVs) are present, see Fig. 2. The CAVs (Veh 1 – Veh 4 in Fig. 2), are indexed in the set $\mathcal{I}^c \subset \mathbb{Z}_+$, while the NCVs (Veh 5 in Fig. 2) are indexed in the set $\mathcal{I}^n \subset \mathbb{Z}_+$, $\mathcal{I}^c \cap \mathcal{I}^n = \emptyset$, and $\mathcal{I} = \mathcal{I}^c \cup \mathcal{I}^n$ is the set of indices for all vehicles. The route
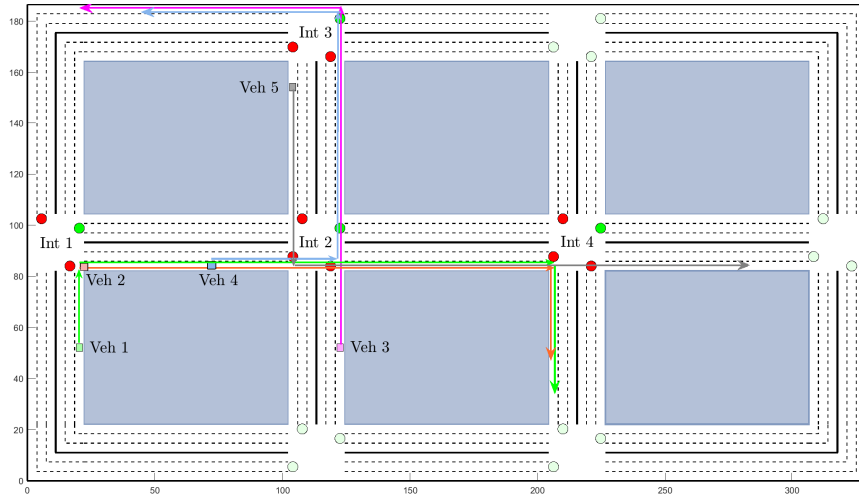
Fig. 2. Scenario including multiple interconnected intersections, traffic lights and CAVs (Veh 1 – Veh 4) and NCV (Veh 5).

for CAVs and NCVs (solid line arrows in Fig. 2) through the map is either known or estimated, at least for a future time interval, the prediction horizon. The prediction horizon may be longer for CAVs than for NCVs, since CAVs typically will provide more route information.

Travel segments are indexed in set $\mathcal{J}^s$ and traffic intersections are indexed in set $\mathcal{J}^\chi \subset \mathbb{Z}_+$, where $\mathcal{J}^s \cap \mathcal{J}^\chi = \emptyset$, and $\mathcal{J} = \mathcal{J}^s \cup \mathcal{J}^\chi$ is the set of indices for all road zones. For intersections $j \in \mathcal{J}^\chi$, multiple crossing directions are possible (see Int 2 in Fig. 2), which are indexed in the set $\mathcal{D}(j) \subset \mathbb{Z}_+$. Similarly, for each segment $j \in \mathcal{J}^s$, multiple travel directions are possible $\mathcal{D}(j) \subset \mathbb{Z}_+$. The index set of lanes in zone $j \in \mathcal{J}$ in direction d is denoted by $\mathcal{S}_\lambda^d(j) \subset \mathbb{Z}_+$.

The CC maximizes the progress of all vehicles towards their goals, by providing motion targets to each CAV and by dynamically adjusting some traffic rules that NCVs obey, here the traffic lights (red/green circles in Fig. 2).

III. Modeling and Problem Definition

For $i \in \mathcal{I}^c$, the ith CAV motion model is

$$x_i(t+1) = f(x_i(t), u_i(t)) \tag{1a}$$
$$p_i(t) = h_p(x_i(t), u_i(t)) \tag{1b}$$
$$\lambda_i(t) = h_\lambda(x_i(t), u_i(t)), \tag{1c}$$

where $x_i \in \mathbb{R}^{r_x^c} \times \mathbb{B}^{b_x^c}$ is the state vector, $u_i \in \mathbb{R}^{r_u^c} \times \mathbb{B}^{b_u^c}$ is the input vector, and f is the state transition function. State and input vectors may include both continuous and binary components. The output functions h_p and h_λ provide the CAV distance traveled from its initial position according to its route $p \in \mathbb{R}_{0+}$ and the CAV lane $\lambda \in \mathbb{Z}_+$, respectively. For each CAV $i \in \mathcal{I}^c$, limits, such as on velocity and acceleration, are imposed by admissible state and input sets

$$x_i \in \mathcal{X}_i, \ u_i \in \mathcal{U}_i. \tag{2}$$

The set $\mathcal{Z}_j^d(i)$, $i \in \mathcal{I}$, $j \in \mathcal{J}$, $d \in \mathcal{D}(j)$ denotes the local positions of vehicle i for which it is in zone j going in direction d, and $z_j^i(p)$ associates to the position p of vehicle i within its route, its global position within zone j, when $p \in \mathcal{Z}_j^d(i)$ for some $d \in \mathcal{D}(j)$.

We also use timers with reset to enable timing constraints, e.g., minimum and maximum between events

$$\tau_\upsilon(t+1) = \begin{cases} \tau_\upsilon(t) + T_s & \text{if} \quad \upsilon(t+1) = \upsilon(t) \\ 0 & \text{if} \quad \upsilon(t+1) \neq \upsilon(t) \end{cases} \tag{3a}$$
$$\mathcal{H}(\upsilon(t+1), \upsilon(t), \tau_\upsilon(t)) \leq 0, \tag{3b}$$

where υ is the triggering variable of the event associated to the timer, T_s is the sampling period, (3a) is the timer update, and (3b) defines the conditions on the next triggering.

The CC controls the traffic light behavior, $\psi_j^d \in \mathbb{B}$ is the variable enabling/disabling passing through the intersection $j \in \mathcal{J}^\chi$, in direction $d \in \mathcal{D}(j)$. The traffic lights must ensure that only one direction is enabled at any time,

$$\bigvee_{d \in \mathcal{D}(j)} \psi_j^d, \quad \forall j \in \mathcal{J}^\chi, \tag{4}$$

and have associated timers $\tau_{\psi_j^d}$ according to (3), where (3b) imposes minimum and maximum switching time,

$$\tau_{\psi_j^d}(t) \leq \tau_{\psi_j^d}^{\min} \implies \psi_j^d(t+1) = \psi_j^d(t) \tag{5a}$$
$$\tau_{\psi_j^d}(t) \geq \tau_{\psi_j^d}^{\max} \implies \psi_j^d(t+1) \neq \psi_j^d(t). \tag{5b}$$

For every vehicle $i \in \mathcal{I}$, the selected lane must be allowed in the current zone $j \in \mathcal{J}$, for the current direction $d \in \mathcal{D}(j)$,

$$p_i \in \mathcal{Z}_j^d(i) \implies \lambda_i \in \mathcal{S}_\lambda^d(j), \tag{6}$$

and lanes may also have an associated timer, τ_{λ_i}, imposing a minimum time between two lane changes,

$$\tau_{\lambda_i}(t) \leq \tau_{\lambda_i}^{\min} \implies \lambda_i(t+1) = \lambda_i(t). \tag{7}$$

Safe crossing through intersection $j \in \mathcal{J}^\chi$ requires,

$$p_i \in \mathcal{Z}_j^d(i) \implies p_{\bar{\imath}} \notin \mathcal{Z}_j^{\bar{d}}(\bar{\imath}), \forall i \neq \bar{\imath}, d \neq \bar{d} \tag{8a}$$
$$\neg \psi_j^d \implies p_i \notin \mathcal{Z}_j^d(i), \tag{8b}$$

where $i, \bar{\imath} \in \mathcal{I}$, $d, \bar{d} \in \mathcal{D}(j)$, and by (8a) only one direction is allowed, while by (8b) traffic cannot cross in a direction not enabled by the traffic light.

Collision avoidance between vehicles is enforced by

$$p_i(t) \in \mathcal{Z}_j^d(i), \ p_{\bar{i}}(t) \in \mathcal{Z}_j^d(\bar{i}), \ z_j^i(p_i(t)) \le z_j^{\bar{i}}(p_{\bar{i}}(t))$$
$$\implies z_j^i(p_i(t+1)) \le z_j^{\bar{i}}(p_{\bar{i}}(t+1))$$
$$\lor \ \lambda_i(t+1) \ne \lambda_{\bar{i}}(t+1), \tag{9}$$

for all $i, \bar{i} \in \mathcal{I}$, $j \in \mathcal{J}$, $d \in \mathcal{D}(j)$, where the left hand side of the implication determines the initial order of two vehicles on the same segment in the same direction, and the right hand side imposes that either the order is maintained, or the vehicles will be in different lanes.

For representing the reactions of NCV $i \in \mathcal{I}^n$ to the, possibly changing, traffic rules, we propose a switched system model. Let $x_i \in \mathbb{R}^{r_x^n} \times \mathbb{B}^{b_x^n}$, $i \in \mathcal{I}^n$, be the NCV state, possibly with both continuous and discrete components, and $X = \{x_i\}_{i \in \mathcal{I}}$, $\Psi = \{\psi_j^d\}_{j \in \mathcal{J}, d \in \mathcal{D}(j)}$, the NCV model is

$$x_i(t+1) = \begin{cases} g_\xi(x_i(t)) & \text{if } \ \mathcal{G}_\xi(X(t), \Psi(t)) \le 0 \\ g_0(x_i(t)) & \text{otherwise} \end{cases} \tag{10a}$$
$$p_i(t) = h_p(x_i(t)) \tag{10b}$$
$$\lambda_i(t) = h_\lambda(x_i(t)), \tag{10c}$$

where h_p, h_λ have the same meaning as for CAVs in (1), g_0 represents the nominal behavior of the NCV when it already complies with the traffic rules, and g_ξ, $\xi \in \Xi \subset \mathbb{Z}_+$ are models for the behaviors imposed by the traffic rules. The switched dynamics g_i enable modeling NCVs behaviors such as stopping at traffic lights, lane changing in case of traffic ahead, collision avoidance, and so on.

Let $\Theta = \{\tau_v\}_{v \in \Upsilon}$ be the set of timers, $P = \{p_i\}_{i \in \mathcal{I}}$, $\Lambda = \{\lambda_i\}_{i \in \mathcal{I}}$, $U = \{u_i\}_{i \in \mathcal{I}^c}$, and consider the cost function

$$J(P_N, \Lambda_N, U_N, \Psi_N) = F\left(P(N|t), \Lambda(N|t), \Psi(N|t)\right) +$$
$$\sum_{k=0}^{N-1} L\left(P(k|t), \Lambda(k|t), U(k|t), \Psi(k|t)\right) \tag{11}$$

over a prediction horizon $N \in \mathbb{Z}_+$, with terminal cost F and stage cost L, where $U_N(t) = (U(0|t), \dots, U(N-1|t))$, and similarly for P_N, Ψ_N, Λ_N. The cost in (11) is not always decomposable among vehicles, since it may model the worst case completion time [4].

Let $X = \{x_i\}_{i \in \mathcal{I}}$ be the set of states for all vehicles and consider the optimal control problem

$$\min_{U_N, \Psi_N} \ J(P_N, \Lambda_N, U_N, \Psi_N) \tag{12a}$$

$$\text{s.t.} \quad (1), (2), \ \forall \ i \in \mathcal{I}^c \tag{12b}$$
$$\hspace{1.2cm} (3), \ \forall \ v \in \Upsilon \tag{12c}$$
$$\hspace{1.2cm} (4), (5), \ \forall \ j \in \mathcal{J}^\chi, \ d \in \mathcal{D}(j) \tag{12d}$$
$$\hspace{1.2cm} (6), (7), \ \forall \ i \in \mathcal{I}^c, \ j \in \mathcal{J}, \ d \in \mathcal{D}(j) \tag{12e}$$
$$\hspace{1.2cm} (8), \ \forall \ i \in \mathcal{I}^c, \ \bar{i} \in \mathcal{I}, \ j \in \mathcal{J}^\chi, \ d, \bar{d} \in \mathcal{D}(j) \tag{12f}$$
$$\hspace{1.2cm} (9), \ \forall \ i \in \mathcal{I}^c, \ \bar{i} \in \mathcal{I}, \ j \in \mathcal{J}, \ d \in \mathcal{D}(j) \tag{12g}$$
$$\hspace{1.2cm} (10), \ \forall \ i \in \mathcal{I}^n \tag{12h}$$
$$\hspace{0.5cm} X(0|t) = X(t), \Theta(0|t) = \Theta(t), \Psi(0|t) = \Psi(t). \tag{12i}$$

Problem 1: At time $t \in \mathbb{R}_{0+}$, given $X(t)$, $\Theta(t)$, $\Psi(t)$, the CC solves (12) to determine the CAVs motion target positions $p_{i,N}^\star(t) = (p_i^\star(0|t), \dots, p_i^\star(N|t))$, for each $i \in \mathcal{I}^c$, and

the traffic light commands $\Psi_N^\star(t) = (\Psi^\star(0|t), \dots, \Psi^\star(N|t))$ as optimal solution to (12). $\qquad\square$

The CC computes the reference velocity commands by (12), but provides only the target positions to each of the CAVs. This enables the on-board CAV guidance to use higher precision models for planning and control [10], to achieve the CC target positions, and to provide other functions such as reactive obstacle avoidance. Next, we discuss an implementation of (12) for specific vehicle motion models and constraint formulations.

IV. Central Coordinator Implementation as MILP/MIQP Formulation

In this section, we briefly present the key steps for implementing the general formulation described in Section III as a mixed-integer linear/quadratic program (MILP/MIQP), for which state of the art solvers [11] exist. In what follows, we drop the time t from the equations when possible, e.g., when all variables refer to the same time step.

A. Controlled Vehicles Modeling

The vehicle longitudinal motion (position p, velocity v) on the road with respect to its start point is represented as a double integrator in closed loop with a velocity controller that tracks a reference velocity command r_i^v, for $i \in \mathcal{I}^c$,

$$p_i(t+1) = p_i(t) + v_i(t)T_s + (K_{\text{LQR}}v_i + Fr_i^v)T_s^2/2, \tag{13a}$$
$$v_i(t+1) = v_i(t) + (K_{\text{LQR}}v_i + Fr_i^v)T_s, \ i \in \mathcal{I}^c. \tag{13b}$$

Here, we compute the stabilizing feedback gain K_{LQR} as an LQR, and the feedforward gain F to achieve unitary dc-gain.

We model the driving lane by a 1-hot encoding vector $\lambda_i \in \mathbb{B}^{n_\lambda}$, where 1 corresponds to the current driving lane for $i \in \mathcal{I}^c$. The lane changes are achieved in one step

$$[\lambda_i(t+1)]_h \iff \begin{array}{l} [\lambda_i(t)]_{h+1} \land \Delta\lambda_i^-(t) \quad \lor \\ [\lambda_i(t)]_{h-1} \land \Delta\lambda_i^+(t) \quad \lor \\ [\lambda_i(t)]_h \land \neg\Delta\lambda_i^+(t) \land \neg\Delta\lambda_i^-(t), \end{array} \tag{14}$$

where $\Delta\lambda_i^+, \Delta\lambda_i^- \in \mathbb{B}$ are the commands to change to the next lane up or down, respectively.

The logical conditions (14) are converted into mixed-integer inequalities using standard methods [12], and together with (2) where the sets are described by polyhedra, and (13), result in generalized mixed-integer linear model for (1)

$$E_i x_i(t+1) \le A_i x_i(t) + B_i u_i(t) + K_i, \tag{15}$$

where $x_i = [p_i \ v_i \ \lambda_i]^\top$, $u_i = [r_i^v \ \Delta\lambda_i^+ \ \Delta\lambda_i^-]^\top$.

B. Dynamic Traffic Rules

The traffic light state $\psi_j^d \in \mathbb{B}$ for intersection $j \in \mathcal{J}^\chi$, in direction $d \in \mathcal{D}(j)$, where 1 corresponds to green, changes by a traffic light change command $\Delta\psi_j^d \in \mathbb{B}$,

$$\psi_j^d(t+1) = \begin{cases} \neg\psi_j^d(t) & \text{if } \quad \Delta\psi_j^d(t) \\ \psi_j^d(t) & \text{if } \quad \neg\Delta\psi_j^d(t) \end{cases} \tag{16}$$

Traffic light update (16) with the safety condition (4) also results in mixed-integer linear inequalities [4].

For implementing the constraint (8), we introduce auxiliary binary variables δ_{ij}^d, $i \in \mathcal{I}$, $j \in \mathcal{J}^\chi$, $d \in \mathcal{D}(j)$ that are membership indicator variables

$$p_i \in [p_{ij}^{\min}, p_{ij}^{\max}] \iff \bigvee_{d \in \mathcal{D}(j)} a_{ij}^d \delta_{ij}^d, \qquad (17)$$

where $p_{ij}^{\min}, p_{ij}^{\max} \in \mathbb{R}_{0+}$ define at what distance on its route vehicle $i \in \mathcal{I}$ enters and exits in zone $j \in \mathcal{J}^\chi$, and $a_{ij}^d \in \mathbb{B}$ defines which direction $d \in \mathcal{D}(j)$ vehicle $i \in \mathcal{I}$ takes in intersection $j \in \mathcal{J}^\chi$, all of which are provided with the route information, and $\sum_{d \in \mathcal{D}(j)} a_{ij}^d = 1$, for all $i \in \mathcal{I}$, $j \in \mathcal{J}^\chi$, and $\sum_{j \in \mathcal{J}^\chi, d \in \mathcal{D}(j)} \delta_{ij}^d \leq 1$, for all $i \in \mathcal{I}$. With the membership variables δ_{ij}^d from (17), we implement (8) as

$$\delta_{ij}^d \implies \psi_j^d, \ \forall i \in \mathcal{I}^c. \qquad (18)$$

Using timers for traffic lights $\tau_{\psi_j^d}$ and lane changes τ_{λ_i}, the minimum and maximum switching time for traffic lights

$$\tau_{\psi_j^d} \leq \tau_{\psi_j^d}^{\min} \implies \neg \Delta \psi_j^d, \quad \tau_{\psi_j^d} \geq \tau_{\psi_j^d}^{\max} \implies \Delta \psi_j^d, \quad (19)$$

and the minimum time between lane changes

$$\tau_{\lambda_i} \leq \tau_{\lambda_i}^{\min} \implies \neg \Delta \lambda_i^- \wedge \neg \Delta \lambda_i^+, \qquad (20)$$

where the timer update equations are (3), and resets are triggered by $\Delta \psi_j^d$, and $\Delta \lambda_i^-$, $\Delta \lambda_i^+$, respectively.

The collision avoidance constraint (9) is formulated as

$$p_i(t) \in \mathcal{Z}_j^d(i) \wedge p_{\bar{\imath}}(t) \in \mathcal{Z}_j^d(\bar{\imath}) \wedge \qquad (21)$$
$$z_j^i(p_i(t)) \leq z_j^{\bar{\imath}}(p_{\bar{\imath}}(t)) \wedge \lambda_i(t+1) = \lambda_{\bar{\imath}}(t+1) \implies$$
$$z_j^i(p_i(t+1)) \leq z_j^{\bar{\imath}}(p_{\bar{\imath}}(t+1)), \ i, \bar{\imath} \in \mathcal{I}, j \in \mathcal{J}, d \in \mathcal{D}(j),$$

for all $i, \bar{\imath} \in \mathcal{I}, i \neq \bar{\imath}, j \in \mathcal{J}$.

Constraints (16)–(21) and the timer update equations (3) involve logical relations among clauses of linear relations among variables, and can be formulated as mixed-integer linear inequalities using standard methods, see, e.g., [12], by introducing auxiliary variables. For the membership constraints, we include auxiliary variables $\delta_{ij}^{\text{in}}, \delta_{ij}^{\text{out}} \in \mathbb{B}$, that are indicators of vehicle $i \in \mathcal{I}$ having passed the beginning and not passed the exit of intersection $j \in \mathcal{J}^\chi$, respectively, while for the collision avoidance constraint (21) we include auxiliary variables $\gamma_{i\bar{\imath}}^{\text{ah}}$, $\gamma_{i\bar{\imath}}^{\text{ln}}$ that are indicators of whether vehicle i is ahead of vehicle $\bar{\imath}$, and that they are in the same lane, respectively, and $\gamma_{i\bar{\imath}j}^{\text{zn}}$ are indicators that vehicles $i, \bar{\imath} \in \mathcal{I}$ are both in zone $j \in \mathcal{J}$, which are defined by membership conditions similar to (17).

C. Switching Dynamic Model for Non-Controlled Vehicles

For the purpose of demonstrating the process, we consider the relatively simple NCV model

$$p_i(t+1) = \begin{cases} b_{ij}^{\min} & \text{if } p_i \in [b_{ij}^{\min}, b_{ij}^{\max}], \\ & \wedge \sum_{d \in \mathcal{D}(j)} a_{ij}^d \psi_j^d = 0 \\ p_i(t) + v_i(t)T_s & \text{otherwise} \end{cases}, \quad (22)$$

where if the traffic light is red and the NCV enters into an area just before the intersection $p_i \in [b_{ij}^{\min}, b_{ij}^{\max}] = [p_{ij}^{\min} - \bar{\beta}, p_{ij}^{\min} - \underline{\beta}]$, $i \in \mathcal{I}^n$, $j \in \mathcal{J}^\chi$, where $\bar{\beta} > \underline{\beta}$ and $\underline{\beta}$ is

arbitrary small, the NCV is going to stop just before the beginning of the intersection. Again, the switched model (22) involves only logics and linear relations. Hence, it can be implemented by mixed-integer linear inequalities with the auxiliary variables μ_{ij}^d that is an indicator of the braking area set membership for the vehicle $i \in \mathcal{I}^n$ approaching the intersection j to be crossed in direction d, variables μ_{ij}^{in}, μ_{ij}^{out} that are indicators of whether the vehicle has passed the beginning and not passed the exit of the braking area, and η_{ij}^d that is an indicator of whether the NCV is in the braking area and the traffic light is red.
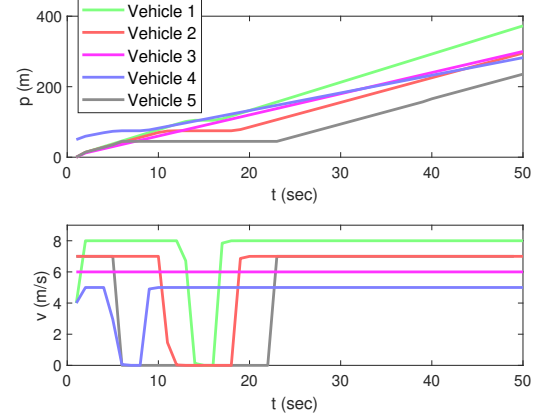
Fig. 3. Position and velocity for all vehicles throughout the simulation across multiple interconnected traffic intersections (see Fig. 2).

D. Cost Function

The desired cost function for the CC is simply maximizing the positions of the vehicles

$$J = \sum_{i \in \mathcal{I}} \sum_{k=1}^{k=N} \|P(k|t) - P^{\text{end}}\|_c + w_1 \|\Lambda(k|t) - \Lambda^{\text{ref}}\|_c$$
$$+ w_2 \|U(k|t) - U^{\text{ref}}\|_c, \quad (23)$$

where $P^{\text{end}} = [p_1^{\text{end}} \ p_2^{\text{end}} \ldots]^\top$ is the vector of final positions in the vehicle routes, and Λ^{ref} and U^{ref} are the desired lane and velocity command vectors, $w_1, w_2 \in \mathbb{R}_{0+}$ are (small) positive weights, $w_1, w_2 \ll 1$, and $c \in \{1, 2, \infty\}$ is chosen to obtain a mixed-integer linear ($c = 1, \infty$) or quadratic ($c = 2$, considering a squared norm) program.

E. Optimization Problem

Based on the implementation in Sec. IV-A–IV-D and depending on the choice of c in (23), (12) results in the mixed-integer linear/quadratic program,

$$\min_\sigma \quad 1/2 \, \sigma^\top Q \sigma + q^\top \sigma \qquad (24a)$$
$$\text{s.t.} \quad H\sigma \leq K \qquad (24b)$$
$$\sigma_\ell \in \{0, 1\}, \ \forall \ell \in \mathcal{B}, \qquad (24c)$$

where the vector of variables σ includes $\{x_i, \tau_{\lambda_i}, u_i\}_i, i \in \mathcal{I}$, $\{\psi_j^d, \Delta\psi_j^d, \tau_{\psi_j^d}\}_{jd}, j \in \mathcal{J}^\chi, d \in \mathcal{D}(j), \{\delta_{ij}^{\text{in}}, \delta_{ij}^{\text{out}}, \delta_{ij}^d\}_{ijd}$, $i \in \mathcal{I}^c, j \in \mathcal{J}^\chi, d \in \mathcal{D}(j), \{\gamma_{i\bar{\imath}}^{\text{ah}}, \gamma_{i\bar{\imath}}^{\text{ln}}, \gamma_{i\bar{\imath}j}^{\text{zn}}\}_{i\bar{\imath}}, i \in \mathcal{I}^c, \bar{\imath} \in \mathcal{I}$,
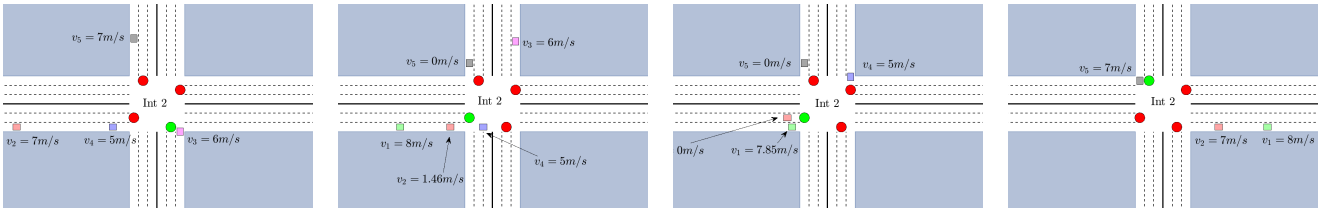
Fig. 4. Snapshots of traffic intersection 2 at different time instants of the closed-loop simulation using the MIP-based central coordinator.

$\{\mu_{ij}^{\text{in}}, \mu_{ij}^{\text{out}}, \mu_{ij}^d, \eta_{ij}^d\}_{ijd}$, $i \in \mathcal{I}^n$, $j \in \mathcal{J}^\chi$, $d \in \mathcal{D}(j)$, and $\mathcal{B}$ denotes the set of indices for binary variables.

While (24) possibly has a large number of binary optimization variables, many do not affect the computational burden because they can be removed by the presolve routine in solvers such as Gurobi [13], or even embedded solvers such as [14], e.g., based on domain propagation for bound strengthening. For example, binary variables for a particular intersection will be removed when that vehicle is traveling far away from that same intersection. Thus, while (24) is large, it can be solved in reasonable time, in practice.

V. SIMULATION RESULTS

We validated the effectiveness of the proposed MIP-based CC in closed-loop receding horizon simulations, on various environments with multiple traffic intersections and multi-lane road segments. Here, we show the results for the environment in Fig. 2, which includes multiple intersections and connecting segments with 3 lanes $[\lambda_i]_1$, $[\lambda_i]_2$, $[\lambda_i]_3$. Vehicles $i = 1, 2, 3, 4$ are CAVs and vehicle $i = 5$ is an NCV. The routing plan information of the vehicles includes initial and final positions, the passing intersections and their crossing directions. The prediction horizon is $N = 10$ and $T_s = 1$s, and we use Gurobi [11] as MIP solver.

Fig. 3 shows the position and velocity for all the vehicles following the route plans shown in Fig. 2 throughout the simulation. The colors in Fig. 3 match those in Fig. 2.

Fig. 4 depicts different snapshots of intersection $j = 2$ at four different times: 1) the traffic light is set to green for vehicle 3 (pink) to cross the intersection in south-north direction; 2) vehicle 3 has passed the intersection, and the traffic light is red, the traffic light in west-east direction is green, vehicle 4 (blue) passes, while the traffic light for the NCV 5 (gray) is red and the vehicle is stopped; 3) since the vehicle 1 (green) with a larger reference velocity gets close to vehicle 2 (red), vehicle 2 changes lane from lane 1 to lane 2 to avoid collision and let vehicle 1 pass; 4) vehicle 2 (red) has changed its lane back, and follows vehicle 1 (green), and since both vehicles have already passed the intersection, the traffic light is turned green for the NCV 5 (gray).

Fig. 5 shows the traffic light indicator ψ_j^d for intersection $j = 2$ for all the 12 possible directions, and the lane change behavior of vehicle $i = 2$. In this simulation, only one direction can cross the intersection at any time, but this can be modified to allow multiple compatible directions to cross the intersection at the same time. The minimum time between
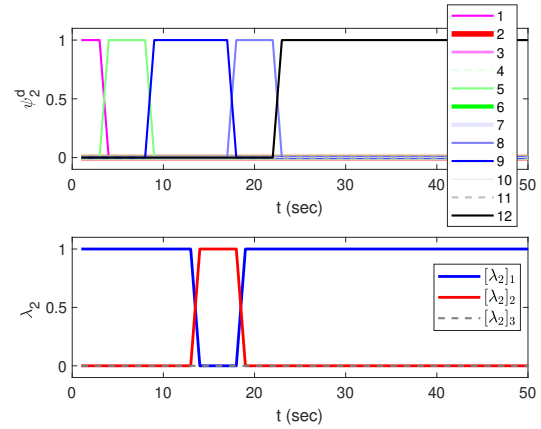

Fig. 5. Top: traffic light variables ψ_2^d, for all directions $d = 1, \ldots, 12$ of intersection 2; the minimum time for the traffic light change is 5s. Bottom: components of the lane change indicator vector λ_2 for vehicle 2.

traffic light changes $\tau_{\psi_j^d}^{\text{min}} = 5$s is satisfied, as is the minimum time between lane changes $\tau_\lambda^{\text{min}} = 5$s.
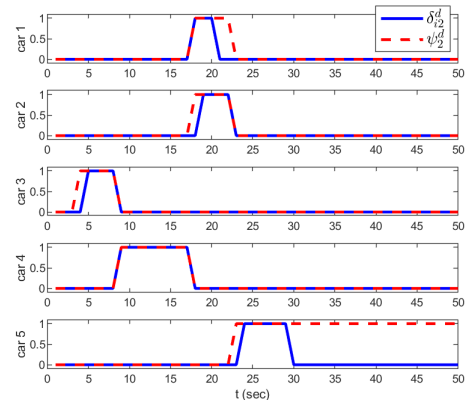

Fig. 6. Binary indicators for intersection membership δ_{ij}^d and corresponding traffic light signal ψ_j^d at intersection $j = 2$ for all vehicles.

Fig. 6 shows δ_{i2}^d and ψ_2^d throughout the entire simulation for all the vehicles crossing intersection $j = 2$ for the actual crossing direction d. Fig. 7 shows the relative distance between vehicle 1 and vehicle 2, $p_2 - p_1$ and the lane indicators for lane 2 for both vehicles $[\lambda_1]_2$, $[\lambda_2]_2$, showing how vehicle 2 changes its lane to avoid collision with vehicle 1 and let it pass. The behavior of the manual vehicle $i = 5$ (gray) in intersection 2 is depicted in Fig. 8. The NCV crosses
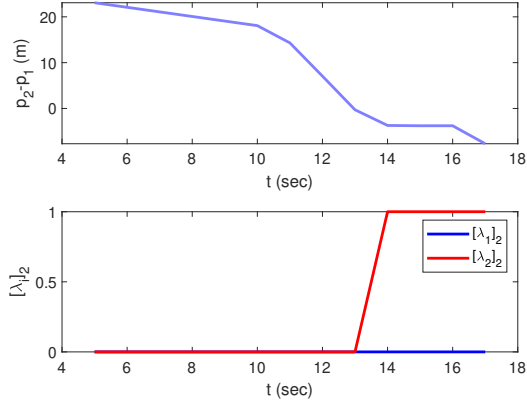
Fig. 7. Top: Relative distance between vehicle 2 and vehicle 1 as they are approaching the intersection 2 (from $t = 5$ s to $t = 17$ s). Bottom: Vehicle 2 changes from lane 1 to lane 2 to let the faster vehicle 1 pass.
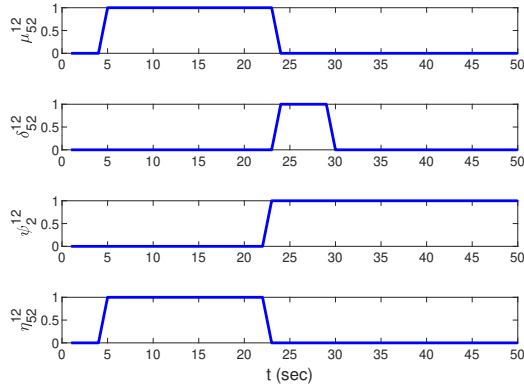

Fig. 8. Variables showing NCV behavior in crossing traffic intersection 2.

intersection 2 in North-South direction, $d = 12$ (see Fig. 2). Fig. 8 shows the set membership indicator for the braking area for vehicle 5, μ_{52}^{12}, the intersection set membership indicator δ_{52}^{12}, the traffic light state ψ_2^{12} that turns green when the vehicle enters the intersection, and the indicator $\eta_{52}^{12} = 1$ if and only if $\mu_{52}^{12} = 1$ and $\psi_2^{12} = 0$.

For the described multi-intersection traffic scenario, the MIP problem (24) has 667 continuous and 6102 binary variables, and 17124 constraints. However, Gurobi uses presolve techniques like domain propagation to reduce the number of variables and it exploits the sparsity in the problem structure to keep the solution time tractable. This is shown in Fig. 9[1], where the maximum computation time is 0.5 s and the average is 0.136 s, which confirms the feasibility of an online implementation in the real application.

VI. CONCLUSIONS

We have proposed a central coordinator (CC) for optimizing the vehicle motion in mixed-traffic situations that directly controls connected automated vehicles (CAVs) by providing

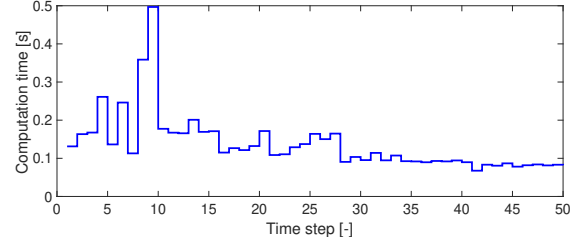[1]Running on a Lenovo T470, with 8GB Ram, Intel i5-7200U, 2.5GHz.

Fig. 9. Gurobi MIP solver computation times in seconds.

targets to the on-board motion planner, and indirectly affects non-controlled vehicles (NCVs) by controlling dynamic traffic rules. The traffic rules are formulated by mixed-logical constraints, and the NCVs prediction model as a switched dynamical system based on such rules. The overall CC optimization problem is formulated as a mixed-integer program, which for a specific subset of rules and models results in an MILP/MIQP that can be solved effectively despite its large dimension due to its structure.

REFERENCES

[1] T. Ersal, I. Kolmanovsky, N. Masoud, N. Ozay, J. Scruggs, R. Vasude-van, and G. Orosz, "Connected and automated road vehicles: state of the art and future challenges," *Vehicle system dynamics*, vol. 58, no. 5, pp. 672–704, 2020.

[2] F. Ye, J. Guo, K. J. Kim, P. V. Orlik, H. Ahn, S. Di Cairano, and M. J. Barth, "Bi-level optimal edge computing model for on-ramp merging in connected vehicle environment," in *Proc. IEEE Intell. Veh. Symp.*, 2019, pp. 2005–2011.

[3] G. Lee, J. Guo, K. J. Kim, P. Orlik, H. Ahn, S. Di Cairano, and W. Saad, "Edge computing for interconnected intersections in internet of vehicles," in *Proc. IEEE Intell. Veh. Symp.*, 2020, pp. 480–486.

[4] S. Ravikumar, R. Quirynen, A. Bhagat, E. Zeino, and S. Di Cairano, "Mixed-integer programming for centralized coordination of connected and automated vehicles in dynamic environment," in *Proc. IEEE Conf. Control Technology and Applications*, 2021.

[5] S. Di Cairano and I. V. Kolmanovsky, "Real-time optimization and model predictive control for aerospace and automotive applications," in *Proc. American Control Conf.*, 2018, pp. 2392–2409.

[6] B. Asadi and A. Vahidi, "Predictive cruise control: Utilizing upcoming traffic signal information for improving fuel economy and reducing trip time," *IEEE Trans. Control Systems Technology*, vol. 19, no. 3, pp. 707–714, 2010.

[7] G. De Nunzio, C. Canudas De Wit, P. Moulin, and D. Di Domenico, "Eco-driving in urban traffic networks using traffic signals information," *Int. J. Robust Nonlinear Control*, vol. 26, no. 6, 2016.

[8] B. De Schutter and B. De Moor, "Optimal traffic light control for a single intersection," *Europ. J. Control*, vol. 4, no. 3, 1998.

[9] X. Liang, X. Du, G. Wang, and Z. Han, "A deep reinforcement learning network for traffic light cycle control," *IEEE Trans. Vehicular Technology*, vol. 68, no. 2, pp. 1243–1253, 2019.

[10] H. Ahn, K. Berntorp, P. Inani, A. J. Ram, and S. Di Cairano, "Reachability-based decision-making for autonomous driving: Theory and experiments," *IEEE Trans. Control Systems Technology*, vol. 29, no. 5, pp. 1907–1921, 2020.

[11] L. Gurobi Optimization, "Gurobi optimizer reference manual," 2021.

[12] V. Raman, A. Donzé, M. Maasoumy, R. M. Murray, A. Sangiovanni-Vincentelli, and S. A. Seshia, "Model predictive control with signal temporal logic specifications," in *Proc. 53rd IEEE Conf. Decision and Control*, 2014, pp. 81–87.

[13] T. Achterberg, R. E. Bixby, Z. Gu, E. Rothberg, and D. Weninger, "Presolve reductions in mixed integer programming," *ZIB Report*, pp. 16–44, 2016.

[14] P. Hespanhol, R. Quirynen, and S. Di Cairano, "A structure exploiting branch-and-bound algorithm for mixed-integer model predictive control," in *Europ. Contr. Conf.*, 2019, pp. 2763–2768.